

Transform Invariant Auto-encoder

Tadashi Matsuo¹, Hiroya Fukuhara² and Nobutaka Shimada³

Abstract—The auto-encoder method is a type of dimensionality reduction method. A mapping from a vector to a descriptor that represents essential information can be automatically generated from a set of vectors without any supervising information. However, an image and its spatially shifted version are encoded into different descriptors by an existing ordinary auto-encoder because each descriptor includes a spatial subpattern and its position. To generate a descriptor representing a spatial subpattern in an image, we need to normalize its spatial position in the images prior to training an ordinary auto-encoder; however, such a normalization is generally difficult for images without obvious standard positions. We propose a transform invariant auto-encoder and an inference model of transform parameters. By the proposed method, we can separate an input into a transform invariant descriptor and transform parameters. The proposed method can be applied to various auto-encoders without requiring any special modules or labeled training samples. By applying it to shift transforms, we can achieve a shift invariant auto-encoder that can extract a typical spatial subpattern independent of its relative position in a window. In addition, we can achieve a model that can infer shift parameters required to restore the input from the typical subpattern. As an example of the proposed method, we demonstrate that a descriptor generated by a shift invariant auto-encoder can represent a typical spatial subpattern. In addition, we demonstrate the imitation of a human hand by a robot hand as an example of a regression based on spatial subpatterns.

I. INTRODUCTION

The auto-encoder method [1], [2], [3] is a type of dimensionality reduction method. It can extract essential information from a vector via general non-linear mapping. Moreover, a mapping from a vector to a descriptor representing essential information can be automatically generated from a set of vectors without any supervising information.

In general, an auto-encoder is generated as an encoder and decoder pair. The encoder converts a vector to a descriptor with lower dimensionality, and the decoder approximately restores the original vector from the descriptor. An auto-encoder can be trained using a set of training samples by minimizing the restoration error of the encoder–decoder combination. After the training, the encoder should be able to generate a numerical representation of the principal components required to restore the original vector. Because the encoder and the decoder can be non-linear and can be trained

without supervisor information, the auto-encoder method is suitable for allocating numerical vectors to targets without simple numerical representations.

As a measure of the accuracy of the restoration performed by a auto-encoder, the simple ℓ^2 measure is often used. Using the ℓ^2 measure, an image and its spatially shifted version are considered to be different. If an auto-encoder is trained with the ℓ^2 measure, images including a common spatial subpattern may be encoded as very different descriptors depending on the position of the subpatterns (Fig. 1(a)). This means that an ordinary auto-encoder inseparably embeds a spatial subpattern and its position within a descriptor. Therefore, to generate a descriptor representing a spatial subpattern in an image, we need to normalize its spatial position in the images prior to training an ordinary auto-encoder. However, such a spatial normalization is generally difficult. For example, the normalization of the appearances of various hand–object interactions such as those shown in Fig. 2, is not obvious and requires a pattern recognition technique to automatically find the standard for each image.

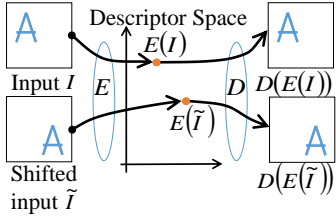
A combination of a convolutional neural network (CNN)[4] and spatial pooling ignores shifts of local small shifts, but it ignores only small shifts. M. Jaderberg et al. proposed “Spatial Transformer Networks” [5], which include a module to learn a spatial transform that is effective in classification. The transform module can cancel a transform including a spatial shift; however it must be trained with a teacher label for each input image. X. Shen et al. proposed “Transform-Invariant Convolutional Neural Networks” [6], but it requires a teacher label for each input image on the training process, too. M. Baccouche et al. proposed “Sparse Shift-Invariant Representation” [7], which requires a special training process where the best translation need to be found for each training sample. M. Ranzato et al. proposed “Sparse and Locally Shift Invariant Feature Extractor”[8]; however, its shift invariance is achieved at the cost of low spatial resolution by down sampling by max-pooling layer.

We propose a transform invariant auto-encoder that outputs a descriptor invariant with respect to a set of transforms. By considering spatial shifts, the proposed method can generate a shift invariant auto-encoder, which extracts a typical spatial subpattern without regard to its relative position in a window (Fig. 1(b)). The proposed method is based on a novel cost function for training an auto-encoder, which induces transform invariance and accurate restoration. The proposed cost function is so designed as to be independent of the concrete structures of an encoder and a decoder of an auto-encoder. Therefore, it can be applied to various auto-encoders without requiring any special modules or labeled training samples.

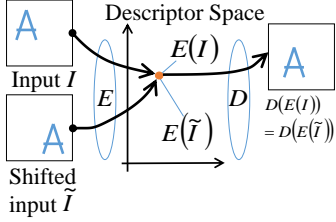
*This work was supported by JSPS KAKENHI Grant Number 24500224, 15H02764 and MEXT-Supported Program for the Strategic Research Foundation at Private Universities, S1311039, 2013-2016.

^{1,3}Tadashi Matsuo and Nobutaka Shimada are with College of Information Science and Engineering, Ritsumeikan University, 1-1-1 Noji-higashi, Kusatsu, Shiga, JAPAN ¹matsuo@i.ci.ritsumei.ac.jp

²Hiroya Fukuhara is with Graduate School of Information Science and Engineering, Ritsumeikan University, 1-1-1 Noji-higashi, Kusatsu, Shiga, JAPAN



(a) An ordinary auto-encoder



(b) A shift invariant auto-encoder

Fig. 1. Characteristics of auto-encoders



Fig. 2. Appearances of hand-object interactions

The proposed method can achieve transform invariance without requiring layers for low spatial resolution. Using the proposed method, we can encode spatial subpatterns in images even if the images are difficult to label or normalize, for example, the appearances of hand-object interactions.

As an example, we have experimented with a shift invariant auto-encoder. In several experiments, we demonstrate that a descriptor using a shift invariant auto-encoder can represent a typical spatial subpattern. We also demonstrate the imitation of a human hand by a robot hand as an example of regression based on spatial subpatterns.

II. ORDINARY AUTO-ENCODER

In general, an auto-encoder is so trained that the encoder-decoder combination approximately restores an input in a certain input set. It is formulated as a problem minimizing a cost function $C_{\text{ord}}(E, D)$ defined as

$$C_{\text{ord}}(E, D) = \sum_{I \in S} \|I - D(E(I))\|_2^2, \quad (1)$$

where S , $D(\cdot)$, $E(\cdot)$, and $\|\cdot\|_p$ denote a set of inputs, the encoder, the decoder, and the ℓ^p norm, respectively.

To minimize $C_{\text{ord}}(E, D)$, the decoder should be able to approximately restore an original vector I from its descriptor $E(I)$, which has a lower dimensionality than I . By training the encoder E and the decoder D by minimizing $C_{\text{ord}}(E, D)$, information sufficient to restore an original vector can be extracted as a descriptor by the encoder. In this way, the auto-encoder method can construct descriptors of vectors from just a set of training vectors.

However, a descriptor of an image from an ordinary auto-encoder includes both a spatial subpattern and its position. If images have a common spatial subpattern at different positions, their descriptors are different.

III. TRANSFORM INVARIANT AUTO-ENCODER

As a method to construct a descriptor representing a property invariant to a certain set of transforms, we propose

a transform invariant auto-encoder. We call the set “ignored transforms”. A transform invariant auto-encoder is generated by training an auto-encoder with a novel cost function. The cost function should induce the accurate restoration of a subpattern as well as transform invariance. We achieve such an cost function by adding a transform variance term and relaxing the restoration error term.

A. Transform Variance Term

As a measure of the transform variance, we propose a sum of differences between a restored image and an image restored from a transformed input as follows:

$$C_{\text{inv}}(E, D) \stackrel{\text{def}}{=} \sum_{I \in S} \sum_i \|D(E(I)) - D(E(T_{\theta_i}(I)))\|_2^2, \quad (2)$$

where S and T_{θ} denote a set of training inputs and a transform operator in the ignored transforms, respectively. To minimize (2), the combination of the encoder E and the decoder D need to output similar vectors for variously transformed versions of an input. By optimizing the encoder E and the decoder D so that they minimize (2), their combination is approximately transform invariant for inputs in the set S .

B. Restoration Error Term

To compare subpatterns without respect to ignored transforms, we need to relax the restoration error cost in (1) so that it will be small if a restored input matches a transformed version of its original input. Therefore, we propose the following term as a measure of the accuracy of the restoration of a subpattern:

$$C_{\text{res}}(E, D) \stackrel{\text{def}}{=} \sum_{I \in S} \min_i \|T_{\theta_i}(I) - D(E(I))\|_2^2. \quad (3)$$

To minimize (3), the restored image $D(E(I))$ should approximately match one of the transformed inputs $\{T_{\theta_i}(I)\}$. This means that the subpattern should be approximately restored.

C. Cost Function

Our total cost function $C(E, D)$ is formulated as follows;

$$C(E, D) \stackrel{\text{def}}{=} \lambda_{\text{inv}} C_{\text{inv}}(E, D) + \lambda_{\text{res}} C_{\text{res}}(E, D) + \lambda_{\text{spa}} \sum_{I \in S} \left(\frac{\|E(I)\|_1}{\|E(I)\|_2} \right)^2, \quad (4)$$

where λ_{inv} , λ_{res} , and λ_{spa} denote the scalar weights of each term. The third term evaluates the spatial sparseness of the descriptors [9].

We train the encoder E and the decoder D so that they minimize the proposed cost function $C(E, D)$.

IV. INFERENCE OF TRANSFORM PARAMETER

We also propose a inference method of a transform parameter which is ignored by a transform invariant auto-encoder. We define a transform parameter of an input I as a parameter representing a transform from the input I to the restored input $D(E(I))$. For example, a transform parameter for a

shift invariant auto-encoder means a spatial shift. An input can be approximately restored from its descriptor and transform parameter. Therefore, a pair of a transform invariant auto-encoder and the corresponding inference model of a transform parameter is an auto-encoder that can represent an input as a pair of a transform invariant part and a transform variant part.

We propose the following cost function to train an inference model R of a transform parameter.

$$C_{\text{par}}(R) = \sum_{I \in S} \left\| R(I) - \underset{\theta}{\operatorname{argmin}} \|I - T_{\theta}(D(E(I)))\|_2^2 \right\|_2^2. \quad (5)$$

We can achieve an inference model R of a transform parameter by minimizing $C_{\text{par}}(R)$.

V. EXPERIMENTS

We demonstrate the effectiveness of the proposed method by experiments with a shift invariant auto-encoder. The shift operator T_{θ_i} is defined as

$$(T_{\theta_i}(I))(x, y) = I(x + \Delta x_i, y + \Delta y_i), \quad (6)$$

where $I(x, y)$ denotes the value of the image I at the position (x, y) . We used the following shift parameters:

$$\{(\Delta x_i, \Delta y_i)\} = \{-8, -6, -4, -2, 0, 2, 4, 6, 8\}^2. \quad (7)$$

A. Experiments for MNIST

Here, we demonstrate shift invariant property of the proposed method using experiments for digit patterns.

As an encoder, we used a neural network consisting of a single CNN with 9×9 filter kernels and 16-channel outputs following a max pooling with stride 2 and a three-layer fully connected neural network (NN), where each layer has 1500, 150, 30 outputs respectively. As a decoder, we used a three-layer fully connected NN, where each layer has 150, 1500, 1024 outputs, respectively. In addition, we used a hyperbolic tangent as an activation function, which is placed between each pair of layers. We generated two pairs of encoders and decoders with the same structure. One was trained as an ordinary auto-encoder by minimizing (1), and the other was trained as a shift invariant auto-encoder by minimizing (4) for digit images of training images in the MNIST database [4]. For the ordinary auto-encoder, we used additional images that were randomly shifted according to the parameters in (7). Both auto-encoders were trained by stochastic gradient descent (SGD) [4] with learning rate 1.0×10^{-3} , and both were updated with every 50 samples that were randomly extracted from the training images (60k samples) in the MNIST database. We used auto-encoders that were updated 100,000 times (≈ 83 epochs). We also trained an inference model R of a shift parameter. The inference model consisted of a three-layer fully connected NN.

As an example, we encoded and decoded an test image of the digit “2”, which is not used in training auto-encoders. Input images are shown in Fig. 3, where the center image is the original image in the MNIST database and the others are its shifted versions. Images in Fig. 4 are restored from images

in Fig. 3 using an ordinary auto-encoder. Images restored by a proposed shift invariant auto-encoder are shown in Fig. 5. Fig. 6 shows the restored images which are shifted according to the shift parameters estimated by the inference model R . In Fig. 4, the restored images are located depending on the shifts in the input images. Conversely, the restored images in Fig. 5 are very similar to each other and they are closer to a typical shape of the digit “2” than the input in Fig. 3. In the cost function (4), there is a trade-off between C_{inv} and C_{res} . In this case, the auto-encoder successfully find a typical shape of the digit “2” by focusing on shapes without their positions.

In addition, we calculated the distributions of the descriptors from the shifted images. We encoded the digit images corresponding to “2”, “5”, and “7” and their shifted versions using the two auto-encoders. Fig. 7 shows the distributions from the ordinary auto-encoder, and Fig. 8 shows those from the shift invariant auto-encoder. In these figures, 30 dimensional descriptors are projected onto a two-dimensional space spanned by the three mean vectors of the descriptors for digits “2”, “5”, and “7”. By comparing these figures, we see that descriptors generated by the shift invariant auto-encoder are obviously concentrated for each digit. With a shift invariant auto-encoder, descriptors from shifted images of the same digit are close to each other and descriptors from shifted images of other digits are far from each other. This means that a descriptor generated by a shift invariant auto-encoder represents the spatial subpattern. In addition, descriptors in Fig. 8 make clusters corresponding to digits, even though we have entered no digit information when training the shift invariant auto-encoder. The proposed method may be applicable to the unsupervised clustering of images based on their spatial subpatterns.

B. Experiments for Hand Object Interactions

Here, we show examples of the encoding appearances of hand-object interactions, which are generally difficult to label or normalize.

In this experiment, we used a two-channel image consisting of a hand region mask and an object region mask (Fig. 9) as the input of the auto-encoders. The structures of the encoder and the decoder are similar to those used in V-A except that the input of the encoder and the output of the decoder are two-channel (32×32)[pixel] interaction images. We generated interaction images from the interaction scene images with a simple background via skin color extraction and background subtraction. We trained an ordinary auto-encoder and a shift invariant auto-encoder with interaction images that included a hand region larger than 20% of the entire image. The interaction images were extracted from random positions of 1680 scenes including the 14 types of interactions shown in Fig. 10. Both auto-encoders were trained using SGD and both were updated with every 168 samples randomly extracted from the 1680 scenes. We used auto-encoders updated 20,000 times.

To compare the spatial patterns represented by the descriptors using an ordinary auto-encoder and a shift invariant auto-

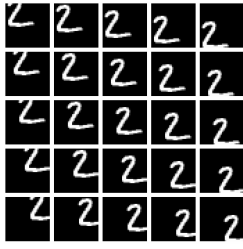


Fig. 3. An image in MNIST and its shifted versions



Fig. 4. Images restored using an ordinary auto-encoder



Fig. 5. Images restored using a shift invariant auto-encoder

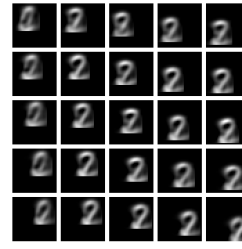


Fig. 6. Images restored using a shift invariant auto-encoder with inferred shifts

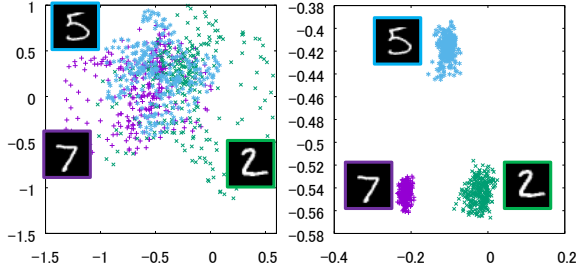


Fig. 7. The distribution of descriptors of shifted images generated by an ordinary auto-encoder

Fig. 8. The distribution of descriptors of shifted images generated by a shift invariant auto-encoder

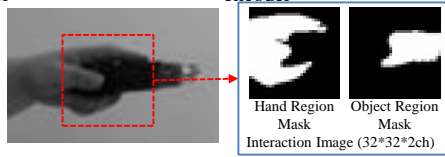


Fig. 9. An interaction image

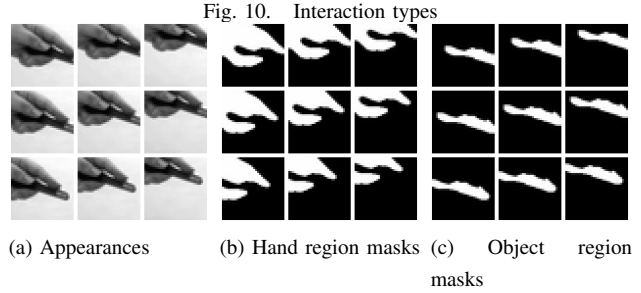
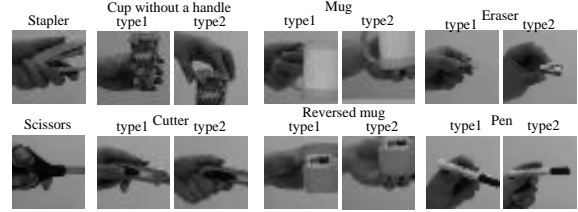


Fig. 11. Example of input interaction images

encoder, we encoded and decoded the interaction images used in the training process. Fig. 11 shows nine interaction images extracted from a scene where a cutter is grasped. Fig. 12 shows the interaction images restored using the ordinary auto-encoder. In the figure, outlines of the restored hand region masks are blurred and differ depending on the shifts in the input images. In particular, the restored images in the right column are very different from their input images. Fig. 13 shows the interaction images restored using the shift invariant auto-encoder. Contrary to the ordinary auto-encoder, the interaction images restored by the shift invariant auto-encoder have clearer outlines. This shows that the descriptors generated by the shift invariant auto-encoder represent spatial subpatterns more accurately than those generated by an ordinary auto-encoder, as we expected.

The restored images are similar to the center image in the left column of Fig. 11. This means that the image is considered to be a typical image in the training process of the shift invariant auto-encoder. In addition, the bottom image in the right column of Fig. 13 is similar to the typical image even though the corresponding input image in Fig. 11 includes only fingertips. This means that a shift invariant auto-encoder can predict a possible neighbor typical pattern

from a local non-typical pattern. The shift invariant auto-encoder enables us to analyze an image using typical features without a dense scan.

In addition, we applied similar experiments to unknown interaction images that are not used in the training process. Fig. 14 shows interaction images restored by the ordinary auto-encoder and the shift invariant auto-encoder. Fig. 14(a) is the case of grasping a cutter, and Fig. 14(b) is the case of grasping scissors. Fig. 14(a) shows that the shift invariant auto-encoder extracted mask shapes regardless of their position. Fig. 14(b) shows that the ordinary auto-encoder failed to restore masks accurately; however, the shift invariant auto-encoder restored typical interaction images. The shift invariant auto-encoder can predict a possible typical interaction image even from images not used in the training process.

C. Experiments on Human Hand Imitation using a Robot Hand

Here, we show examples using the proposed method for controlling a robot hand. Even though a joint angle can be represented numerically, it is not obvious which combinations of joint angles of a robot hand are effective for grasping an object. If a robot hand can imitate the effective hand posture of a human, the cost of designing the joint angles

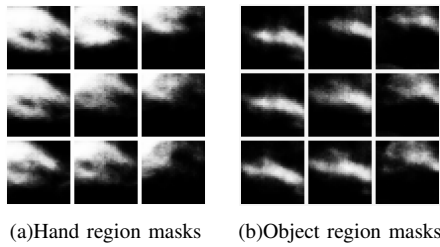


Fig. 12. Interaction images restored using an ordinary auto-encoder

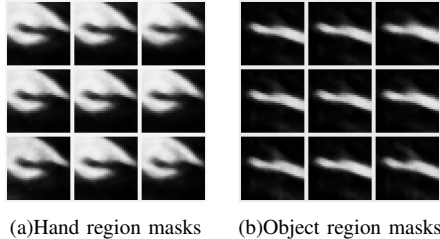


Fig. 13. Interaction images restored using a shift invariant auto-encoder

can be reduced. Such imitations can be realized by learning the relationship between the appearance of a human hand and the corresponding joint angles of a robot hand. A shift invariant auto-encoder can effectively numerically represent the appearance of a human hand because the corresponding joint angles of a robot hand are independent of the location of the human hand in the view.

We developed an imitation program as follows.

- 1) Collect depth images of postures of a human hand.
- 2) Generate a shift invariant auto-encoder for the collected depth images.
- 3) Allocate the joint angles of a robot hand to several postures of a human hand.
- 4) Train a neural network regressor to calculate the joint angles of a robot hand from a descriptor of a human hand posture.

Using a shift invariant auto-encoder, we can generate a descriptor representing a human hand shape directly from the appearances without any normalization.

In this experiment, we used a 3-finger robot hand with 10 degrees of freedom (9 DOF fingers and 1 DOF wrist). We trained a shift invariant auto-encoder and a regressor so that the fingers of the robot hand imitated the thumb, the forefinger and the middle finger (Fig. 15). The encoder of the shift invariant auto-encoder consists of two CNN layers and a three-layer fully connected NN, and the decoder is a three-layer fully connected NN. In this experiment, the encoder converts a single channel (32×32)[pixel] depth image into a 100-dimensional descriptor and the regressor converts a descriptor into the joint angles of the robot hand. The shift invariant auto-encoder is trained with 9377 depth images and the regressor is trained with 1339 pairs of descriptors and manually determined combinations of joint angles.

To demonstrate the effectiveness of the proposed method, we developed a similar program using principal component analysis (PCA) instead of the shift invariant auto-encoder. The dimension of the descriptors used by the PCA is 100,

which is the same as that used by the shift invariant auto-encoder. The cumulative contribution ratio for the dimension is approximately 95%.

The left two columns in Fig. 16 show RGB images and depth images of a human hand that are not used in the training process. The third and fifth columns in the figure show images restored by the shift invariant auto-encoder and PCA, respectively. The shapes of the fingers are preserved in the images restored by the shift invariant auto-encoder; however, PCA does not preserve such features. This is because a descriptor generated by PCA depends on the position of the spatial subpattern and the positions of the human hand in Fig. 16 are different from the training samples. This means that the shift invariant auto-encoder is more suitable for generating a descriptor representing a spatial subpattern.

We show the results of the imitations in the fourth and sixth columns in Fig. 16, where the robot hand replays the joint angles calculated by the regressor. In the case using PCA (the sixth column in Fig. 16), the joint angles of the robot hand are very different from those of the human hand. However, in the case using the shift invariant auto-encoder (the fourth column in Fig. 16), the joint angles of the three fingers of the robot hand appear similar to those of the human hand. Because a descriptor generated by the shift invariant auto-encoder represents the spatial shape accurately, the regressor can learn the relationship between a shape and the joint angles more accurately than when using PCA.

In Fig. 17, we show error histograms for 9 joints on fingers and a joint on the wrist. They are calculated from 27 samples that are not used in the training process. In Fig. 17, “PCA+NN” and “SIAE+NN” mean NN-based angle regressions from a descriptor by PCA or Shift Invariant Auto-Encoder (SIAE). “Direct CNN” means a CNN-based direct regression from an input image to joint angles without intermediate descriptors. In Fig. 17(a), the histograms are similar, but Fig. 17(b) shows that the SIAE+NN estimated the wrist angles more accurately than the PCA+NN and the Direct CNN. The PCA+NN and the Direct CNN may be overfitted to the training samples. The root mean squared errors (RMSEs) of the PCA+NN, the Direct CNN and the SIAE+NN for fingers are 30.8, 22.2 and 22.1[degree], respectively. The RMSEs of them for the wrist are 64.2, 49.0 and 56.2[degree], respectively. Although the SIAE+NN has a larger RMSE due to a few samples with very large error, the ratio of samples with errors within ± 5 [degree] is 81% much larger than 22% (the PCA) and 11% (the Direct CNN) as shown in Fig. 17(b).

These results show that a shift invariant auto-encoder is effective for regression based on a spatial subpattern.

VI. CONCLUSIONS

We proposed a transform invariant auto-encoder and demonstrated that a shift invariant auto-encoder can generate a descriptor representing a spatial subpattern regardless of its position. In several experiments, we showed that the

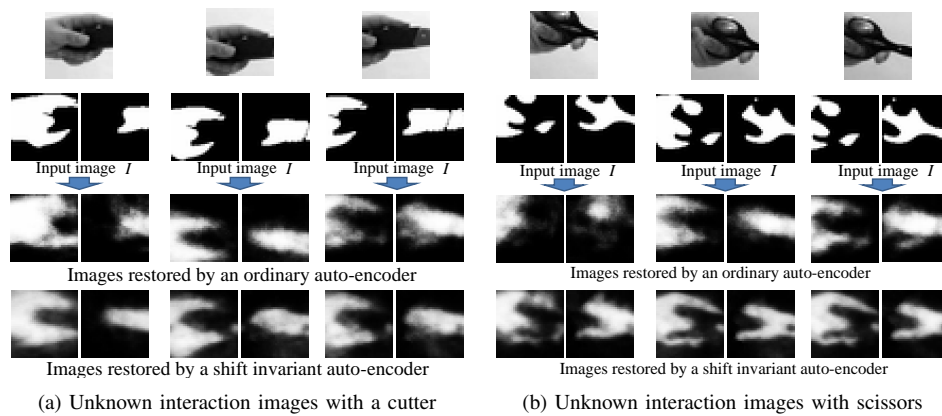


Fig. 14. Restoration from unknown interaction images

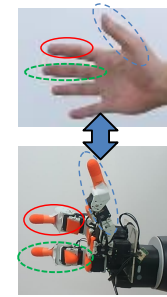


Fig. 15. Correspondence of the human hand to the robot hand

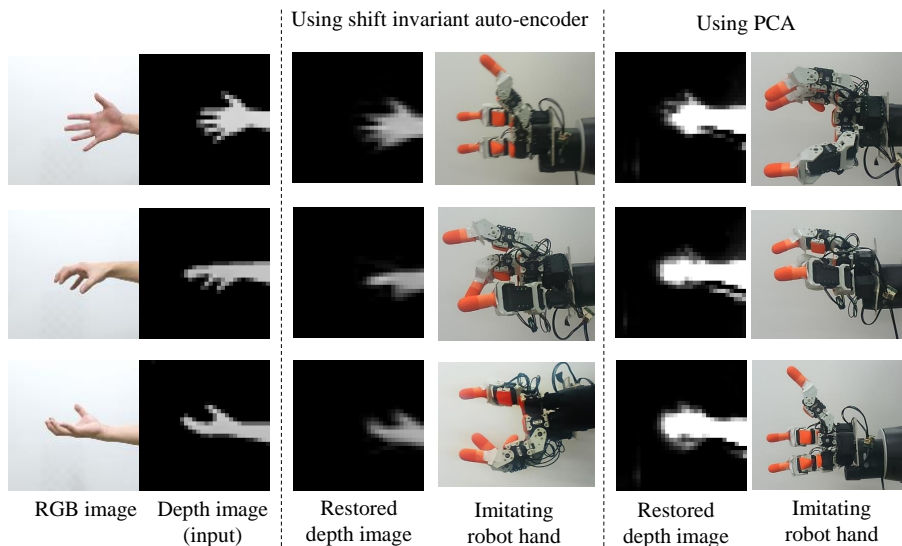


Fig. 16. Imitation of a human hand by a robot hand

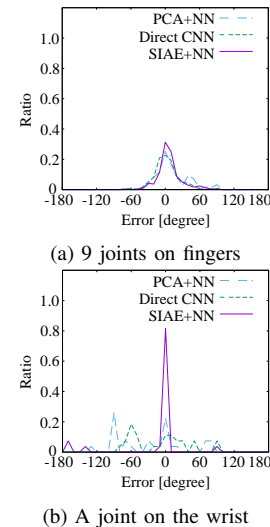


Fig. 17. Error histograms of estimated joint angles

proposed method is applicable to regression based on a spatial subpattern.

In this paper, we experimented with spatial subpatterns and shifts. However, the framework of the proposed cost function can be applied to temporal patterns and other transforms such as dilation and rotation. Since the proposed function requires enumeration of transforms, random sampling of transforms may be required to suppress the computation cost. With such an extension, an auto-encoder will be able to independently encode typical motions in a video without regard to dilation and rotation. This will be useful for motion-based recognition.

REFERENCES

- [1] P. Baldi and K. Hornik, "Neural networks and principal component analysis: Learning from examples without local minima," *Neural Networks*, vol. 2, no. 1, pp. 53 – 58, 1989. [Online]. Available: <http://www.sciencedirect.com/science/article/pii/0893608089900142>
- [2] G. E. Hinton and R. R. Salakhutdinov, "Reducing the dimensionality of data with neural networks," *Science*, vol. 313, no. 5786, pp. 504–507, 2006. [Online]. Available: <http://science.sciencemag.org/content/313/5786/504>
- [3] A. Makhzani and B. J. Frey, "k-sparse autoencoders," *CoRR*, vol. abs/1312.5663, 2013. [Online]. Available: <http://arxiv.org/abs/1312.5663>
- [4] Y. Lecun, L. Bottou, Y. Bengio, and P. Haffner, "Gradient-based learning applied to document recognition," *Proceedings of the IEEE*, vol. 86, no. 11, pp. 2278–2324, Nov 1998.
- [5] M. Jaderberg, K. Simonyan, A. Zisserman, and K. Kavukcuoglu, "Spatial transformer networks," *CoRR*, vol. abs/1506.02025, 2015. [Online]. Available: <http://arxiv.org/abs/1506.02025>
- [6] X. Shen, X. Tian, A. He, S. Sun, and D. Tao, "Transform-invariant convolutional neural networks for image classification and search," in *Proceedings of the 2016 ACM on Multimedia Conference*, ser. MM '16. New York, NY, USA: ACM, 2016, pp. 1345–1354. [Online]. Available: <http://doi.acm.org/10.1145/2964284.2964316>
- [7] M. Baccouche, F. Mamalet, C. Wolf, C. Garcia, and A. Baskurt, "Sparse shift-invariant representation of local 2d patterns and sequence learning for human action recognition," in *Pattern Recognition (ICPR), 2012 21st International Conference on*, Nov 2012, pp. 3823–3826.
- [8] M. Ranzato and Y. LeCun, "A sparse and locally shift invariant feature extractor applied to document images," in *Ninth International Conference on Document Analysis and Recognition (ICDAR 2007)*, vol. 2, Sept 2007, pp. 1213–1217.
- [9] T. Matsuo and N. Shimada, "Construction of latent descriptor space of hand-object interaction," in *Proceedings of 22nd Japan-Korea Joint Workshop on Frontiers*, Feb. 2016, pp. 117–122.